Spectroscopy and Electrochemistry of Cobalt(III) Schiff Base Complexes

Arnd Böttcher, Toshihiko Takeuchi, Kenneth I. Hardcastle,† Thomas J. Meade, and Harry B. Gray*

Beckman Institute, California Institute of Technology, Pasadena, California 91125

Dory Cwikel, Moshe Kapon, and Zvi Dori

Department of Chemistry, Technion-Israel Institute of Technology, Technion City, Haifa 32000, Israel

Received September 18, 1996[⊗]

The structural, spectroscopic, and electrochemical properties of cobalt(III) derivatives of acacen (H_2acacen = bis(acetylacetone) ethylenediimine) and related ligands have been investigated. Electronic structure calculations indicate that the absorption between 340 and 378 nm in Co^{III}(acacen) spectra is attributable to the lowest $\pi-\pi^*$ intraligand charge-transfer transition. Equatorial ligand substitutions affect reduction potentials less than axial ligand changes, consistent with an electronic structural model in which d_{z^2} is populated in forming cobalt(II). The crystal structure of [Co(3-Cl-acacen)$(NH_3)_2$]BPh_4 has been determined: The compound crystallizes in the monoclinic space group $P2_1/m$ (No. 11) with $a = 9.720(2)$ Å, $b = 18.142(4)$ Å, $c = 10.046(2)$ Å, $\beta = 100.11(3)°$, $D_c = 1.339$ g cm^{-3}, and $Z = 2$; the complex cation, [Co(3-Cl-acacen)$(NH_3)_2$]$^+$, exhibits a slightly distorted octahedral coordination geometry. The distances between the cobalt atom and the two axial nitrogen donor atoms differ only slightly (1.960(6) and 1.951(6) Å) and are similar to Co−N distances found in cobalt−ammine complexes as well as the axial Co−N distances in [Co(acacen)(4-MeIm)$_2$]Br·1.5H_2O; the latter compound crystallizes in the triclinic space group $P\bar{1}$ (No. 2) with $a = 18.466(9)$ Å, $b = 14.936(7)$ Å, $c = 10.111(5)$Å, $\alpha = 96.27(5)°$, $\beta = 94.12(5)°$, $\gamma = 112.78(5)°$, $D_c = 1.447$ g cm^{-3}, and $Z = 4$.

Introduction

A milestone in the use of metals in medicine was the introduction of *cis*-dichlorodiammineplatinum(II) (cisplatin) as an anticancer drug.[1,2] As a result of extensive basic research, a great deal is now known about the modes of binding of platinum(II) complexes to biological molecules and the likely mechanisms of cisplatin antitumor activity. Much less is known, however, about the antitumor and, in some cases, antiviral properties of other metal complexes.[1]

The discovery that certain cobalt(III) Schiff base complexes are potent antiviral agents prompted us to initiate an investigation of Co(III) interactions with proteins and nucleic acids.[3,4] Since complexes with relatively labile axial ligands exhibit higher activities, we suspect that axial binding of Co(III) to biological targets is somehow involved in the mechanism (or mechanisms) of action. Accordingly, in parallel with experiments aimed at assessing their modes of binding with biomolecules, we have measured absorption spectra[5] and reduction potentials[6] of a series of Co^{III}(acacen) (H_2acacen = bis(acetylacetone) ethylenediimine) complexes with the goal of evaluating the effects of axial ligation (X) and equatorial substitution (A, B) on electronic properties (Figure 1). In the course of our work, we determined the structures of [Co(3-Cl-acacen)$(NH_3)_2$]BPh_4 (**16**) (H_2(3-Cl-acacen) = bis(3-chloroacetylacetone) ethylenediimine) and [Co(acacen)(4-MeIm)$_2$]Br·1.5H_2O (**17**); these are the first reported structures of Co(acacen) complexes containing neutral N-donor axial ligands.

Experimental Section

Materials. All chemicals used were of reagent grade. Ethylenediamine and 3-chloro-2,4-pentanedione were obtained from Aldrich, $CoCl_2$·6H_2O was from EM Science, and tetra-*n*-butylammonium tetrafluoroborate (electrochemical grade) was from SACHEM. Acetonitrile (Omnisolv solvent) was from EM Science, nitromethane was purchased from Fluka, and absolute ethanol was from Quantum Chemical Corp. Complexes **1**−**17** were synthesized according to procedures described by Dori et al.[7] The following description of the synthesis of [Co(3-Cl-acacen)$(NH_3)_2$]Cl is given as an example.

[Co(3-Cl-acacen)$(NH_3)_2$]Cl. A solution of 6 g (0.1 mol) of ethylenediamine in 50 mL of absolute ethanol was slowly added (dropwise) to a solution of 26.9 g (0.2 mol) of freshly distilled 3-chloro-2,4-pentanedione in 150 mL of absolute ethanol over a period of 2 h at room temperature. During this time a white precipitate was formed. The reaction mixture was stirred for an additional 3 h and filtered.

†Department of Chemistry, California State University, Northridge, CA 91330.

⊗ Abstract published in *Advance ACS Abstracts,* April 15, 1997.

(1) Lippard, S. J. In *Bioinorganic Chemistry*; Bertini, I., Gray, H. B., Lippard, S. J., Valentine, J. S., Eds.; University Science Books: Mill Valley, CA, 1994; p 505.
(2) Bloemink, M. J.; Reedijk, J. In *Metal Ions in Biological Systems*; Sigel, A., Sigel, H., Eds.; Marcel Dekker, Inc.: New York, 1996; p 641. Whitehead, J. P., Lippard, S. J. *Ibid.,* p 687.
(3) (a) Dunkel, E. C., Geary, P. A., Brooks, J., Pavan-Langsion, D. *4th Int. Conf. on Antiviral Res.* **1991,** 170 (New Orleans, LA). **(**b) Devlin, H.; Geary, P.; Pavanlangston, D.; Dori, Z.; Dunkel, E. C. *Inv. Ophth-V* **1993**, *34,* 1348.
(4) Böttcher, A.; Takeuchi, T.; Simon, M. I.; Meade, T. J.; Gray, H. B. *J. Inorg. Biochem.* **1995**, *59,* 221.
(5) Reports of Co^{III}(acacen) absorption spectra: (a) Marcu, G.; Várhelyi, C.; Fülöp, J.; Itul, D. *Rev. Roum. Chim.* **1989**, *34,* 1029. (b) Abdel Salam El Absy, M.; Marcu, G.; Zsakó, J.; Várhelyi, C. *Rev. Roum. Chim.* **1982**, *27,* 917. (c) Costa, G.; Mestroni, G.; Tauzher, G.; Stefani, L. *J. Organomet. Chem.* **1966**, *6,* 181.
(6) Reports of Co^{III}(acacen) electrochemistry: (a) Averill, D. F.; Broman, R. F. *Inorg. Chem.* **1978**, *17,* 3389. (b) Costes, J. P.; Cros, G.; Muratet, F.; Darbieu, M.-H. *Polyhedron* **1987**, *6,* 995. (c) Costes, J. P.; Cros, G.; Darbieu, M.-H.; Laurent, J.-P. *Trans. Met. Chem.* **1982**, *7,* 219. (d) Darbieu, M.-H.; Cros, G.; de Montauzon, D.; Laurent, J.-P. *Trans. Met. Chem.* **1982**, *7,* 149. (e) Costa, G.; Mestroni, G.; Puxeddu, A.; Reisenhofer, E. *J. Chem. Soc. A* **1970**, 2870.
(7) Dori, Z.; Gershon, D.; Tivon, K. Metallo-Organic Salt Compounds and Pharmaceutical Uses Thereof. U.S. Patent No. 5,049,557, Sept 1991.

S0020-1669(96)01146-9 CCC: $14.00

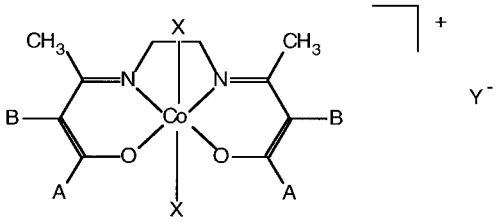

Complex	A	B	X	Y
1	Me	H	NH_3	Cl
2	Ph	H	NH_3	Cl
3	Me	Cl	NH_3	Cl
4	Ph	Cl	NH_3	Br
5	Me	H	py	Br
6	Ph	H	py	Br
7	Me	H	Im	Cl
8	p-ClPh	H	NH_3	Br
9	p-FPh	H	NH_3	PF_6
10	p-MeOPh	H	NH_3	Br
11	Me	H	N-MeIm	Br
12	Me	H	2-MeIm	Br
13	Ph	H	Im	Br
14	Me	Cl	2-MeIm	Br
15	Ph	Cl	2-MeIm	Br
16	Me	Cl	NH_3	BPh_4
17	Me	H	4-MeIm	Br

Figure 1. Cobalt(III) acacen complexes.

The colorless crystals of H_2(3-Cl-acacen) were washed three times with water and then with diethyl ether and dried over $CaCl_2$ (5.7 g, 19.4%). ^{1}H NMR (300 MHz, $CDCl_3$): δ = 2.20 (s, CH_3), 2.32 (s, CH_3), 3.54 (s, CH_2), 11.41 (s, NH).

To a solution of 2.05 g (7.0 mmol) of H_2(3-Cl-acacen) in 50 mL of methanol was added 1.66 g (7.2 mmol) of solid $CoCl_2 \cdot 6H_2O$ under nitrogen. The blue solution was heated with stirring for 30 min. A saturated solution of NH_3 in methanol (1 mL) was added slowly, and the reaction mixture was refluxed for another 1 h. After this time 10 mL of NH_3-saturated methanol was added and oxygen was bubbled slowly through the solution. The reaction mixture was stirred overnight at room temperature. During this time brown crystals of [Co(3-Cl-acacen)$(NH_3)_2$]Cl formed. The crystals were filtered out, washed with cold methanol and then with diethyl ether, and dried over $CaCl_2$ (2.25 g, 77%). Anal. Calcd for [Co(3-Cl-acacen)$(NH_3)_2$]Cl·H_2O ($C_{12}H_{22}Cl_2CoN_4O_2$): C, 32.94; H, 5.53; N, 12.80. Found: C, 33.37; H, 5.65; N, 12.79. IR (cm^{-1}, KBr): ν(C=N) 1625. ^{1}H NMR (300 MHz, D_2O): δ = 2.34 (s, CH_3), 2.52 (s, CH_3), 3.76 (s, CH_2).

[Co(3-Cl-acacen)$(NH_3)_2$]Cl was converted to [Co(3-Cl-acacen)-$(NH_3)_2$]BPh_4 by adding a saturated solution (excess) of $KBPh_4$ in methanol to an aqueous solution of [Co(3-Cl-acacen)$(NH_3)_2$]Cl. The precipitate was filtered out and dried (yield: 91%).

Methods. Electronic absorption spectra were recorded on a Hewlett Packard HP 8452 diode array spectrophotometer. ^{1}H NMR spectra were obtained on a GE QE 300 MHz NMR spectrometer in $CDCl_3$ or D_2O with the solvent as internal reference. IR spectra were recorded as KBr pellets on a Perkin-Elmer Model 1600 FT-IR spectrometer. Elemental analyses were obtained at the Caltech analytical facility.

Cyclic voltammetry was performed using an EG&G Princeton Applied Research Model 173 potentiostat/galvanostat driven by a Model 175 universal programmer and equipped with a standard three-electrode configuration. A Ag/AgCl electrode containing 3 M NaCl (BAS MF 2063) served as reference electrode, a Pt wire as counter electrode, and a glassy carbon electrode as working electrode. Cyclic voltammetric measurements were performed at 20 °C under argon in acetonitrile with 0.1 M tetra-*n*-butylammonium tetrafluoroborate as the supporting electrolyte. The solvent was passed through activated alumina prior to use. Potentials are reported vs Ag/AgCl in 3 M NaCl. Ferrocene was added after each run as an internal standard. The Fe(II/III) couple of ferrocene was observed at 0.450 V under these experimental conditions (scan rate = 0.1 V/s) . The complex concentration was ≈ 1 mM.

Table 1. Crystallographic Data for [Co(3-Cl-acacen)$(NH_3)_2$]BPh_4[a]

formula	$C_{36}H_{42}BCl_2CoN_4O_2$
M_n	703.38
color	brownish
shape	irregular
cryst system	monoclinic
space group	$P2_1/m$
a, Å	9.720(2)
b, Å	18.142(4)
c, Å	10.046(2)
β, deg	100.11(3)
V, Å^3	1744.0(6)
Z	2
D_{calc}, g cm^{-3}	1.339
radiation	Mo Kα
wavelength, Å	0.710 73
μ, cm^{-1}	6.83
temp, K	293(2)
cryst size, mm	0.18 × 0.30 × 0.38
diffractometer	Enraf-Nonius CAD-4
collcn method	ω scans
θ range, deg	2.06−19.98
reflcns collcd	3851
indepdt reflcns	1694
reflcns used	1692
F(000)	736
R_{int}	0.033
$R(F)$[a]	0.062
$R_w(F^2)$[b]	0.110
$(\Delta/\sigma)_{max}$	0.003
goodness of fit	2.64

[a] $R(F) = \sum||F_o| - |F_c||/\sum|F_o|$. [b] $R_w(F^2) = \{\sum[w(F_o^2 - F_c^2)^2]/\sum wF_o^4\}^{1/2}$, where $w = 1/[\sigma^2(F_o^2)]$.

Crystal Structure Analysis of [Co(3-Cl-acacen)$(NH_3)_2$]BPh_4. Crystals of [Co(3-Cl-acacen)$(NH_3)_2$]BPh_4 suitable for X-ray crystallography were grown by slow evaporation from a nitromethane solution at room temperature. Cell dimensions and intensity data were measured with an Enraf-Nonius CAD-4 diffractometer using monochromated Mo Kα radiation. Cell dimensions were determined by least-squares refinement of 25 reflections with 2θ angles from 16−20°. Three control reflections showed a loss of intensity of 0.28% during data collection. A linear decay correction was applied to the data in addition to the Lorentz and polarization corrections. No absorption correction was applied. Atom scattering factors and values for $\Delta f'$ and $\Delta f''$ were taken from Cromer[8] and Cromer and Waber,[9] and CRYM,[10] SHELXS-86,[11] SHELXL-93,[12] and XP/PC[13] computer programs were used for data processing, solution, refinement, and tables.

The structure was solved by direct methods using SHELXS-86 and refined using full-matrix least-squares techniques. The atomic positions for C(4) and C(4b) were found by difference Fourier synthesis, and all the hydrogen atoms were placed in their expected chemical positions, except for those on N(2) and N(3), which were positioned by calculating the electron density around the nitrogen atoms and fitting the H atom positions to the highest electron density peaks. Final difference Fourier maps showed largest residuals of +0.445 and −0.460 e Å^{-3}. A summary of data collection and structure refinement is given in Table 1; atomic coordinates are given in Table 2.

(8) Cromer, D. T. *International Tables for X-ray Crystallography*; Kynoch Press: Birmingham, U.K., 1974; Vol. IV, pp 149−151.
(9) Cromer, D. T.; Waber, J. T. *International Tables for X-ray Crystallography*; Kynoch Press: Birmingham, U.K., 1974; Vol. IV, pp 99−101.
(10) Duchamp, D. J. In *Abstracts of Papers*, American Crystallographic Association Meeting, Bozeman, MT, 1964; Paper B14, p 29.
(11) Sheldrick, G. M. *Acta Crystallogr.* **1990**, *A46*, 467.
(12) Sheldrick, G. M. Program for Structure Refinement, University of Göttingen, Germany, 1993.
(13) XP/PC, Molecular Graphics Software, Siemens Analytical X-Ray Instruments, Inc., Madison, WI.

Table 2. Atomic Coordinates ($\times 10^4$) and Equivalent Isotropic Displacement Parameters ($Å^2 \times 10^3$) for $[Co(3\text{-Cl-acacen})(NH_3)_2]BPh_4$[a]

atom	*x*	*y*	*z*	*U*(eq)
Co	1660(1)	2500	6173(1)	49(1)
O(1)	2459(4)	1804(3)	5148(4)	57(1)
N(1)	881	1778	7179	76(2)
N(1b)	881	3222	7179	76(2)
N(2)	3428(6)	2500	7442(6)	59(2)
N(3)	−34(6)	2500	4790(6)	67(2)
Cl(1)	1657(4)	−216(1)	5991(3)	193(2)
C(1)	2371(8)	1098(5)	5217(8)	73(2)
C(2)	1606(11)	741(4)	6088(12)	97(3)
C(3)	919(9)	1086(5)	7027(8)	91(3)
C(4)	449	2025	8433	91(3)
C(4b)	−36	2789	7974	91(3)
C(5)	155(10)	586(6)	7897(9)	190(6)
C(6)	3177(8)	703(4)	4274(8)	112(3)
C(20)	−4130(7)	1793(3)	351(6)	49(2)
C(21)	−5402(7)	1494(4)	580(7)	64(2)
C(22)	−6096(8)	936(5)	−200(9)	86(3)
C(23)	−5574(11)	652(5)	−1263(10)	95(3)
C(24)	−4349(10)	919(5)	−1554(7)	80(2)
C(25)	−3636(7)	1490(4)	−765(7)	62(2)
C(40)	−1681(9)	2500	1299(8)	51(3)
C(41)	−891(7)	1853(4)	1451(5)	59(2)
C(42)	563(8)	1850(5)	1736(6)	75(2)
C(43)	1299(12)	2500	1877(10)	87(4)
C(30)	−3573(8)	2500	2777(9)	52(3)
C(31)	−3557(7)	1856(4)	3527(7)	68(2)
C(32)	−3522(7)	1849(5)	4923(7)	84(3)
C(33)	−3529(10)	2500	5611(11)	83(4)
B	−3390(11)	2500	1196(10)	45(3)

[a] *U*(eq) is defined as one-third of the trace of the orthogonalized $\mathbf{U}_{ij}$ tensor.

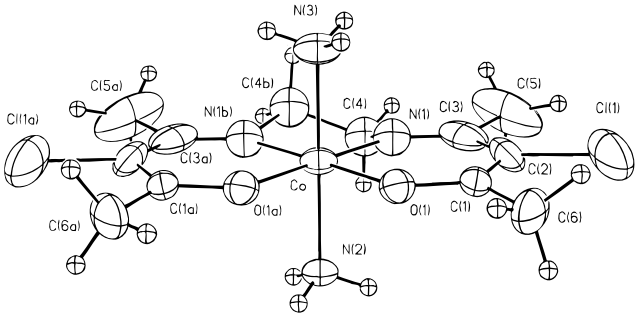

Figure 2. Molecular structure (plot with 30% probability ellipsoids) of $[Co(3\text{-Cl-acacen})(NH_3)_2]BPh_4$ (cation only) showing the atomic labeling scheme.

We have also determined the structure of a very similar cobalt cation complex, $[Co(acacen)(4\text{-MeIm})_2]Br\cdot 1.5H_2O$, differing primarily in the axial ligands; it is included in this paper for comparison. Complete details of structural results including bond distances and angles are given in the Supporting Information.

Results and Discussion

Structures. Crystal structure analysis confirms the expected octahedral coordination geometry of the complex cation, $[Co(3\text{-Cl-acacen})(NH_3)_2]^+$; Figure 2 shows the molecular structure with the atomic labeling scheme. Selected bond lengths and angles are given in Table 3. The tetradentate Schiff base ligand (ONNO ligand) coordinates the cobalt atom in a planar fashion with two ammonia molecules occupying the axial positions of the complex. The octahedral coordination polyhedron is slightly distorted, where all angles around the cobalt center deviate significantly from 90°. The values of the Co−O and Co−N bond lengths in the equatorial ligand plane are 1.881(4) and 1.892(1) Å, respectively. The distances between the cobalt atom and the two axial nitrogen donor atoms differ only slightly

Table 3. Selected Bond Distances (Å) and Bond Angles (deg) in $[Co(3\text{-Cl-acacen})(NH_3)_2]BPh_4$

Distances[a]			
Co−N(1)	1.8918(9)	O(1)−C(1)	1.286(8)
Co−N(2)	1.951(6)	C(1)−C(6)	1.512(9)
Co−N(3)	1.960(6)	C(3)−C(5)	1.538(10)
Co−O(1)	1.881(4)	N(1)−C(4)	1.4655(3)
N(1)−C(3)	1.267(10)	N(1b)−C(4b)[b]	1.5152(3)
C(2)−C(3)	1.396(11)	C(4)−C(4b)	1.5102(3)
C(1)−C(2)	1.403(11)	Cl(1)−C(2)	1.740(8)

Angles[a]			
N(1)−Co−N(1b)	87.58(5)	N(1)−Co−N(2)	92.3(2)
O(1)−Co−N(1)	94.06(14)	O(1)−Co−N(2)	87.5(2)
O(1)−Co−O(1a)[b]	84.3(3)	O(I)−Co−N(3)	89.3(2)
O(1a)−Co−N(1)[b]	94.06(14)	N(1)−Co−N(3)	90.74(14)

[a] Atomic numbering shown in Figure 2. [b] Symmetry transformations used to generate equivalent atoms: x, $-y + {}^1/_2$, z (see comments in Results and Discussion).

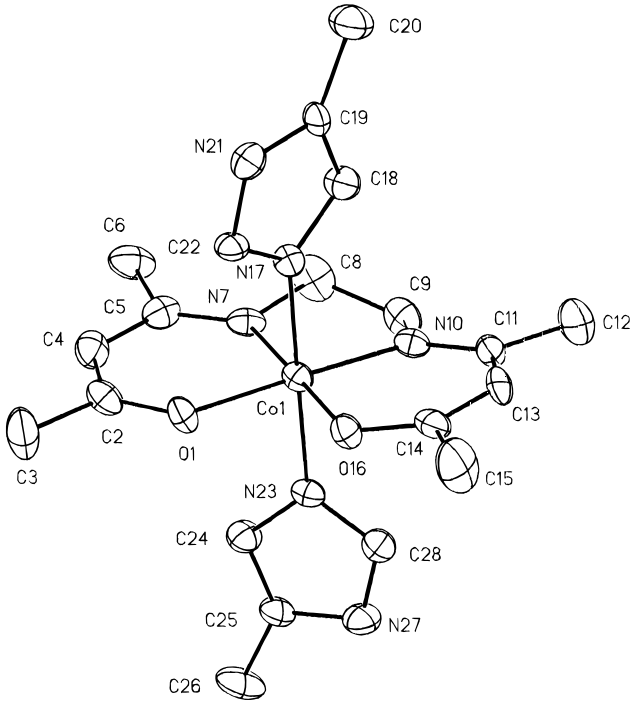

Figure 3. Molecular structure (plot with 30% probability ellipsoids) of $[Co(acacen)(4MeIm)_2]Br\cdot 1.5H_2O$ (cation only) showing the atomic labeling scheme.

(1.960(6) and 1.951(6) Å) and compare well with the Co−N distances found in cobalt−ammine complexes (e.g., $[Co(NH_3)_6]Cl_3$ (Co−N = 1.963 Å).[14]

The O−Co−N angles in the equatorial plane are larger than 90° (94.06°), and the O−Co−O and N−Co−N angles smaller than 90° (84.3 and 87.6°, respectively). The average bond distances and angles for Co−N (equatorial and axial) and Co−O in $[Co(acacen)(4\text{-MeIm})_2]^+$ are the same (within 3σ) as the corresponding values in $[Co(3\text{-Cl-acacen})(NH_3)_2]^+$. Figure 3 shows the molecular structure and atomic labeling scheme for one of the two unique cations in the asymmetric unit in $[Co(acacen)(4\text{-MeIm})_2]Br\cdot 1.5H_2O$. The planar complex $[Co^{II}(acacen)]$[15] also exhibits approximately the same bond angles around the metal center; however, the Co−O and Co−N bond distances are significantly shorter (average Co−O and C-N bond lengths: 1.853 and 1.874 Å, respectively) than those in the Co(III) analogue, owing to the absence of axial ligands.

(14) Krüger, G. J.; Reynhardt, E. C. *Acta Crystallogr.* **1978**, *B34*, 915.
(15) Brückner, S.; Calligaris, M.; Nardin, G.; Randaccio, L. *Inorg. Chim. Acta* **1968**, *2* (4), 386.

Two related structures with anionic axial ligands, [Co(acacen)(py)(N_3)][16] and K[Co(acacen)gly_2]·6H_2O (gly = glycinato),[17] have been reported. The bond angles around the metal compare well with the values determined for [Co(3-Cl-acacen)-(NH_3)$_2$]BPh_4; however, the average Co−O and Co−N distances in the equatorial plane (Co−N = 1.914, Co−O = 1.903 Å in [Co(acacen)(py)(N_3)]; Co−N = 1.897, Co−O = 1.907 Å in K[Co(acacen)gly_2]·6 H_2O) as well as the distances between the Co atom and the axial ligands (Co−N(py) = 1.980, Co−N(azide) = 1.952 Å in [Co(acacen)(py)(N_3)]; Co−N(gly) = 1.979 and 1.966 Å, respectively, in K[Co(acacen)gly_2]·6H_2O) are significantly greater in these complexes.

The cation and anion are located on crystallographic mirror planes (although the cation does not possess a mirror plane), and since the cobalt atom is at a special position, refinement in a higher symmetry space group was required. Anisotropic refinement of the structure indicated a slight rotational disorder about the N(2)−Co−N(3) axis and also indicated disorder in the ethylene bridge, which is indeed found for a number of related crystal structures of Schiff base complexes. However, the gauche conformation of the ethylene bridge is clearly more stable.[15] Therefore, the principal conformation of C(4) and C(4b) was determined from a difference Fourier map calculated using the complete cation less C(4) and constrained during final refinements. The bond distances N(1)−C(4) and N(1b)−C(4b) are most likely not different and should have higher errors, but the imposed crystallographic symmetry complicated the final refinements.

Electronic Spectroscopy. The absorption spectrum of H_2-acacen features an intense band system with maxima at 305 and 323 nm ($\epsilon \approx 30\,000$ M^{-1} cm^{-1});[5c] the splitting in the system has been attributed to the coupling of the two azomethine chromophores.[18] A higher energy system with a band maximum at 196 nm ($\epsilon \approx 7800$ M^{-1} cm^{-1}) also is observed. In the corresponding phenyl-substituted ligand (A = Ph), absorption bands are observed at 350 ($\epsilon \approx 34\,000$) and 243 nm ($\epsilon \approx 19\,000$ M^{-1} cm^{-1}).[6a] The bands at lower energy are attributable to $\pi-\pi^*$ transitions associated with the azomethine chromophore, and the band at higher energy arises from $\pi-\pi^*$ transitions within the phenyl rings. In contrast to the Schiff base H_2salen (bis(salicylaldehyde) ethylenediimine), no n → π^* band is observed in the H_2acacen spectrum; in the case of H_2acacen, the 305/323 nm system is only slightly shifted in acidic solution.[19]

The cobalt(III)acacen complexes exhibit absorption peaks that are red-shifted approximately 30−50 nm relative to those of their respective uncomplexed ligands (Figure 4); in each case an intraligand transition of the conjugated system gives rise to an intense feature between 218 and 260 nm ($\epsilon \approx 15\,000-35\,000$ M^{-1} cm^{-1}) (Table 4). The $\pi-\pi^*$ absorptions of the complexes with a phenyl substituent in position A occur at lower energies ($\lambda_{max} > 248$ nm) and are more intense ($\epsilon \approx 30\,000$ M^{-1} cm^{-1}) than those of the complexes containing a less extended conjugated system (A = Me; $\lambda_{max} = 218-248$ nm; $\epsilon \approx 20\,000$ M^{-1} cm^{-1}). The complexes with A = phenyl show an additional weaker band at about 300 nm ($\epsilon \approx 7000-15\,000$ M^{-1} cm^{-1}), which can be assigned to the first allowed $\pi-\pi^*$ transition in the aromatic rings. Some of the observed bands are partially obscured by $\pi-\pi^*$ transitions of the aromatic systems of complexes containing either pyridine or imidazole derivatives as axial ligands.

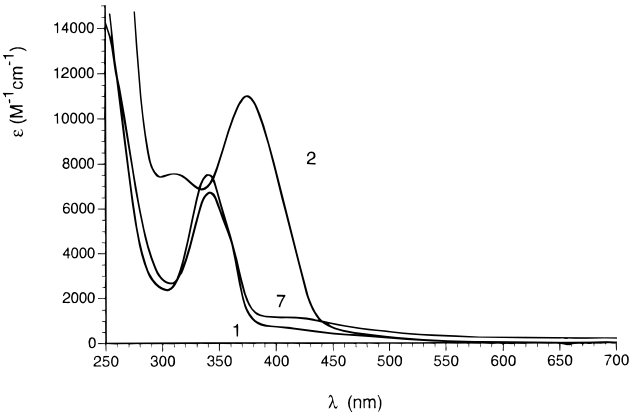

Figure 4. Electronic absorption spectra of [Co(acacen)$(X)_2$]Y complexes in acetonitrile solution (T = 293 K, d = 1 cm, $c = 1 \times 10^{-4}$ M): **1**, [Co(acacen)$(NH_3)_2$]Cl; **2**, [Co(1-Ph-acacen)$(NH_3)_2$]Cl; **7**, [Co(acacen)$(Im)_2$]Cl.

The most prominent feature in the near-UV region of the Co^{III}-(acacen) spectra in acetonitrile solution is a band between 340 and 378 nm ($\epsilon \approx 6500-16\,600$ M^{-1} cm^{-1}) attributable to a $\pi-\pi^*$ intraligand transition.[20] In each complex the band is red-shifted by about 30 nm from the corresponding absorption in the free ligand. Similar free ligand to complex red shifts are observed in the spectra of zinc(II) and nickel(II) salen complexes.[21]

The assignment of the near-UV band as a $\pi-\pi^*$ intraligand charge-transfer transition is supported by electronic structure calculations employing an INDO/s semiempirical method developed and optimized for spectroscopic predictions by Zerner and co-workers.[22] The calculation predicts that metallation of the free ligand will red-shift the transition and reduce its oscillator strength, as observed. Changing A from methyl to phenyl results in extended conjugation, further lowering the transition energy, while increasing the oscillator strength considerably. Although the calculated absolute energies of the transitions are higher than the experimental energies, the trends are consistent with the experiments.[23] The HOMO in the transition is centered at the carbon atom bonded to substituent B; the LUMO is an antibonding orbital located mainly on the C and N atoms that form the imine bond.

Two shoulders are observed on the low-energy side of the near-UV band. In the spectra of complexes **6**, **9**, **10**, and **13**, the 350 nm maximum appears to be split into two components, as in the free ligand, with a weak shoulder at slightly lower energy. The axial ligand X does not have any significant influence on the position of this band (see, for example,

(16) Clearfield, A.; Gopal, R.; Kline, R. J.; Sipski, M.; Urban, L. O. *J. Coord. Chem.* **1978**, *7*, 163.
(17) Holbrook, S. R.; van der Helm, D. *Acta Crystallogr.* **1975**, *B31*, 1653.
(18) Larsen, E. *Acta Chem. Scand.* **1969**, *23*, 2158.
(19) The corresponding Co(II) complex [Co(acacen)] shows absorption bands at 218 ($\epsilon \approx 22\,000$), 294 ($\epsilon \approx 10\,200$), 336 ($\epsilon \approx 5000$), and 376 nm ($\epsilon \approx 3700$ M^{-1} cm^{-1}).[5c]
(20) This band is shifted to shorter wavelengths by 5−12 nm in aqueous solution. Substitution of the counteranion of the complex (chloride, bromide, tetraphenylborate) does not significantly influence the spectrum.
(21) Bosnich, B. *J. Am. Chem. Soc.* **1968**, *90*, 627.
(22) a) Ridley, J. E.; Zerner, M. C. *Theor. Chim. Acta* **1973**, *32*, 111. (b) Bacon, A.; Zerner, M. C. *Theor. Chim. Acta* **1979**, *53*, 21. (c) Zerner, M. C.; Loew, G. H.; Kirchner, R. F.; Mueller-Westerhoff, U. T. *J. Am. Chem. Soc.* **1980**, *102*, 589. (d) Edwards, W. D.; Weiner, B.; Zerner, M. C. *J. Phys. Chem.* **1988**, *92*, 6188.
(23) The Argus program was used for the calculations. Dreiding force fields were used to minimize any changes made to the periphery of the ligand, but all other ligand atoms were fixed in position. In order to calculate the effect of changes in the intraligand charge-transfer band, the cobalt atom was replaced by zinc and the axial ligands were removed. Results are as follows [$\pi-\pi^*$ energy, cm^{-1} (oscillator strength, A)]: Free ligand (L), A = Me, B = H, 40 049 (0.9366); Zn(L), A = Me, B = H, 36 314 (0.8972); Zn(L), A = Ph, B = H, 35 083 (1.197).

Table 4. Electronic Absorption Data for $[Co(acacen)(X)_2]Y$ in Acetonitrile Solution[a]

No.	A	B	X	Y	λ, nm (ϵ, M^{-1} cm^{-1})					
1	Me	H	NH_3	Cl		341 (7500)	358 (5100) sh	402 (700) sh	466 (357) sh	590 (40) sh
2	Ph	H	NH_3	Cl	310 (7550)	375 (11 000)	412 (5300) sh	440 (1000) sh	628 (63) sh	692 (42) sh
3	Me	Cl	NH_3	Cl		356 (7050)	370 (5500) sh	414 (900) sh	592 (89) sh	694 (37) sh
4	Ph	Cl	NH_3	Br		368 (8200)	378 (7700) sh	440 (950) sh		710 (17) sh
5	Me	H	py	Br		340 (6500)	356 (4700) sh	440 (730)		
6	Ph	H	py	Br		369 (11 500)	404 (6200) sh[b]	440 (1450) sh		
7	Me	H	Im	Cl		343 (6700)	358 (4900) sh	408 (1000)	480 (535) sh	
8	p-ClPh	H	NH_3	Br	308 (9600)	379 (12 500)	418 (5900) sh	450 (1000) sh		
9	p-FPh	H	NH_3	PF_6	298 (9600)	374 (13 400)	404 (8000) sh[c]	446 (1200) sh		
10	p-MeOPh	H	NH_3	Br	312 (14 700)	367 (16 600)	402 (9700) sh[d]	454 (850) sh		
11	Me	H	*N*-MeIm	Br		342 (6600)	356 (4900) sh	414 (770)		
12	Me	H	2-MeIm	Br		338 (7300)	356 (4700) sh	436 (650)	644 (89) sh	
13	Ph	H	Im	Br		376 (10 700)	404 (7000) sh[e]	444 (1270) sh		
14	Me	Cl	2-MeIm	Br		349 (7300)	374 (4300) sh	442 (760)	628 (63) sh	
15	Ph	H	2-MeIm	Br		367 (10 300)	404 (5800) sh	438 (1700) sh		

[a] $T = 293$ K, $d = 1$ cm, $c = 1 \times 10^{-4}$ or 1×10^{-3} M. [b−e]Additional shoulders observed as follows: [b]382 (10 200); [c]382 (12 700); [d]382 (14 800); [e]384 (10 300).

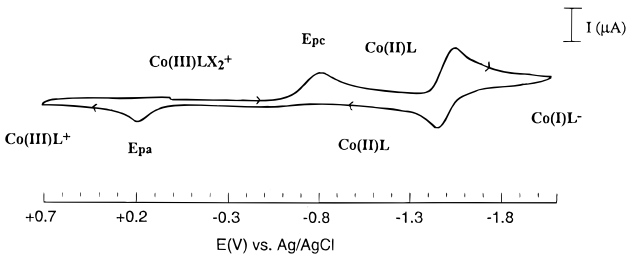

Figure 5. Cyclic voltammogram of $[Co(3\text{-Cl-acacen})(NH_3)_2]Cl$ (**3**) in acetonitrile at 293 K. Scan rate: 100 mV/s.

complexes **1**, **5**, **7**, **11**, and **12**); however, substitution of H by Cl in position B of the complexes shifts the band to higher wavelengths, and the same is true for the introduction of phenyl substituents in position A of the ligand. In the latter case, the position of the absorption maximum depends on the para-substituents on the phenyl rings. Electron-withdrawing substituents shift the band to even lower energy (complex **8**), while electron-donating substituents cause blue shifts (complex **10**).

The shoulder on the low-energy side of the 350 nm band ($\epsilon \approx 5000$ M^{-1} cm^{-1}), which was found to be only poorly resolved in several complexes, is not strongly affected by the axial ligands. The shoulder is shifted by the different substituents on the ligand framework in the same fashion as described above. In contrast, the band in the 400−450 nm region, which is a shoulder in most complexes and a true maximum in only five cases (complexes **5**, **7**, **11**, **12**, and **14**), is significantly influenced by the axial ligands X. The energy of this transition decreases in the order NH_3 > Im > N-MeIm > 2-MeIm > py (A = Me). A similar trend (exception: *N*-MeIm) is observed for the corresponding Co(III/II) reduction potentials.

Electrochemistry. A typical cyclic voltammogram of a Co^{III}-(acacen) complex in the potential range from 0.7 to −2.1 V (vs Ag/AgCl) in acetonitrile solution is shown in Figure 5. A scan initiated in the negative direction at 0.0 V reveals a first irreversible reduction wave at ca. −0.8 V, which is due to the process $[Co^{III}L(X)_2]^+ + e^- \rightarrow [Co^{II}L] + 2X$. The reduction of the Co(III) complex results in the loss of its axial ligands in weakly coordinating solvents, since the electron is added to the antibonding d_{z^2} orbital.[24]

A second, well-defined reversible process at ca. −1.6 V is observed with about unit ratio of anodic to cathodic peak currents (i_{pa}/i_{pc}), corresponding to the simple one-electron process $[Co^{II}L] + e^- \rightarrow [Co^{I}L]^-$.[26] Upon reversal of the scan direction, the Co(II) complex is reoxidized to Co(III) at much higher potentials (ca. 0.2 V). Then, in a rapid consecutive reaction, the six-coordinate species $[Co^{III}L(X)_2]^+$ is formed again (i.e., the electron transfer is followed by a chemical reaction), since upon scan reversal and scanning through a second cycle no cathodic wave is observed for this electrode process; reduction occurs at the same potential (≈−0.8 V) as observed in the first cycle. Multiple scans resulted in nearly superposable cyclic voltammograms, thereby showing the marked stability of the three oxidation states of cobalt involved in the electrochemical study.

Figure 6 shows the effect of pyridine concentration on the electrochemical behavior of $[Co^{II}(acacen)]$: In the absence of pyridine, the quasi-reversible Co(III/II) couple is observed at 0.155 V. Upon addition of 1 equiv of pyridine, the anodic wave is broadened and oxidation occurs at slightly lower potential, whereas the reduction wave is shifted by more than 700 mV in the negative direction (complex **5**, Table 5). With increasing pyridine concentration, the anodic peak potential is cathodically shifted (indicating increased formation of five-coordinate pyridine adducts; i.e., the electrode process is preceded by a reversible chemical reaction: $[Co^{II}L] + X \rightleftarrows [Co^{II}L(X)]$), whereas the corresponding cathodic reduction potential remains constant. At high pyridine concentrations, the Co(III/II) redox couple becomes quasi-reversible.[27] In contrast, the Co(II/I) couple is not significantly affected by the concentration of pyridine present in solution.

(24) Equilibrium constants for the reaction $[Co^{II}L] + X \rightleftarrows [Co^{II}L(X)]$ have been estimated to fall in the range 100−1000 M^{-1};[25] i.e., if the axial ligand is not present in excess, the corresponding four-coordinate Co(II) complex will be the dominant species in solution. Indeed, the reversible Co(II/I) couple does not depend on the concentration of the potential axial ligands, which confirms that the Co(III) complex loses both axial ligands upon electrochemical reduction to Co(II) in acetonitrile solution under the experimental conditions.

(25) Carter, M. J.; Rillema, D. P.; Basolo, F. *J. Am. Chem. Soc.* **1974**, *96*, 392.

(26) The anodic−cathodic peak potential separation for the Co(II/I) couple is 75−95 mV (scan rate 0.1 V/s) and thus larger than expected theoretically for a reversible one-electron process: Bard, A. J.; Faulkner, L. R. *Electrochemical Methods, Fundamentals and Applications*; Wiley: New York, 1980. However, under the conditions of our experiment the peak separation of the ferrocene/ferrocenium couple was observed to be 80−100 mV, which can be used as a criterion for electrochemical reversibility. The peak separation increases only slightly with increasing scan rate, and the same is true for the ferrocene/ferrocenium couple under our experimental conditions.

(27) In neat pyridine, where the cobalt(II) complex is apparently five-coordinate, the Co(III/II) couple for the complex $[Co^{II}(acacen)]$ was observed to be reversible ($E = -0.59$ V vs SCE (potential for the anodic wave, determined by polarography)),[25] which means that the bis(pyridine) adduct $[Co^{II}L(X)_2]$ must be present at the surface of the electrode in equilibrium with the corresponding Co(III) species; thus the earlier conclusion[25] that $Co^{II}(acacen)$ complexes form only mono-(pyridine) adducts requires revision.

Table 5. Reduction Potentials (in V) of [Co(acacen)$(X)_2$]Y in Acetonitrile Solution[a]

complex	A	B	X	Y	E_{pa}(II → III)[b]	E_{pc}(III → II)[c]	$E_{1/2}$(II ⇔ I)[d]
1	Me	H	NH_3	Cl	0.150	−1.040	−1.77
2	Ph	H	NH_3	Cl	0.240	−0.970	−1.57
3	Me	Cl	NH_3	Cl	0.145	−0.815	−1.51
4	Ph	Cl	NH_3	Br	0.340	−0.830	−1.39
5	Me	H	py	Br	0.185	−0.710	−1.78
6	Ph	H	py	Br	0.220	−0.670	−1.58
7	Me	H	Im	Cl	0.230	−0.975	−1.78
8	p-ClPh	H	NH_3	Br	0.210	−0.880	−1.54
9	p-FPh	H	NH_3	PF_6	0.240	−0.910	−1.57
10	p-MeOPh	H	NH_3	Br	0.195	−0.940	−1.63
11	Me	H	N-MeIm	Br	0.125	−1.075	−1.78
12	Me	H	2-MeIm	Br	0.295	−0.855	−1.77
13	Ph	H	Im	Br	0.275	−0.925	−1.60
14	Me	Cl	2-MeIm	Br	0.255	−0.690	−1.51
15	Ph	H	2-MeIm	Br	0.210	−0.775	−1.58

[a] Potentials are vs Ag/AgCl in 3 M NaCl, $T = 293$ K, $c = 1 \times 10^{-3}$ M, $\nu = 100$ mV/s. [b] Anodic peak potential for the process $[Co^{II}L] \rightarrow [Co^{III}L]^+ + e^-$. [c] Cathodic peak potential for the process $[Co^{III}L(X)_2)]^+ + e^- \rightarrow [Co^{II}L] + 2X$. [d] Formal potential for the reversible process $[Co^{II}L] + e^- \leftrightarrow [Co^{I}L]$.

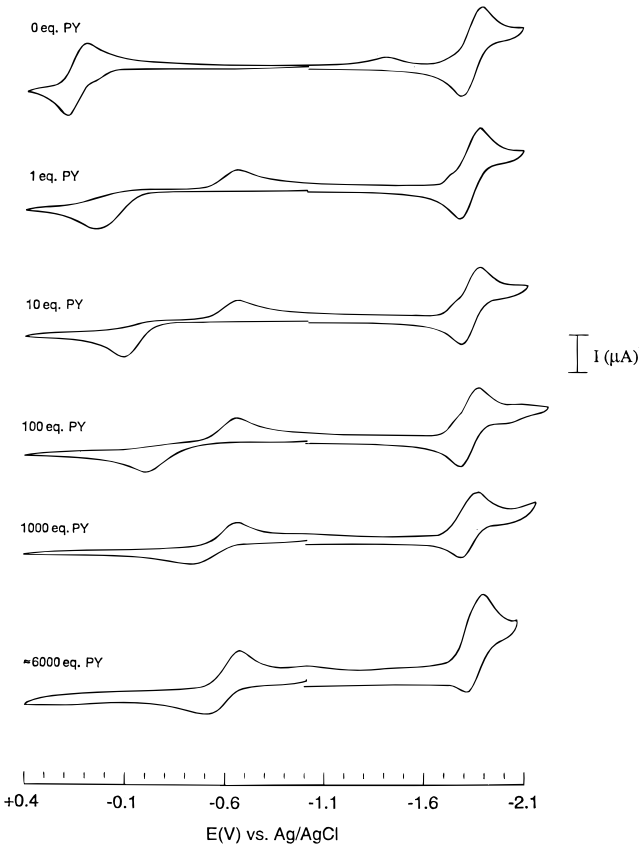

Figure 6. Cyclic voltammograms of $[Co^{II}(acacen)]$ at different pyridine concentrations at 293 K. Scan rate: 100 mV/s.

The reduction potentials for the different complexes are set out in Table 5. The formal potentials for the reversible Co(II/I) redox couple were calculated as the average of the cathodic (E_{pc}) and anodic (E_{pa}) peak potentials of this process; the potentials given for the oxidation of Co(II) and the reduction of Co(III) are the respective peak potentials.

The observed anodic peak potentials I_{pa} for the reduction process Co(III) + e^- → Co(II) depend strongly on the nature of the axial ligand X (differing by almost 400 mV) and are related to the σ-donor strength of the respective axial ligand in a qualitative manner; the electron affinity of the Co(III) complex decreases with increasing pK_a of the axial Lewis base.[28]

For the complexes with A = Me, complex **11** (X = *N*-MeIm) is the most difficult to reduce ($E = -1.075$ V); reduction of the corresponding bis(pyridine) analogue occurs at −0.71 V. An explanation of the very cathodic potential of complex **11** is not yet at hand; however, the order found for complexes **5** (X = py), **7** (X = Im), and **1** (X = NH_3) correlates nicely with increasing electron density on the cobalt center caused by the increasing basicity of the ligands. The more positive potential of **12** (X = 2-MeIm) compared to complex **7** with the less basic axial imidazole suggests longer metal−N(2-MeIm) distances and therefore less electron density on the cobalt center in the former complex; it is likely that axial elongation is caused by steric repulsions involving the methyl group of 2-MeIm.

The σ-donor strength of the different axial ligands is also reflected in the spectra of the complexes: The energy of the transition between 402 and 440 nm decreases in the order NH_3 > Im > N-MeIm > 2-MeIm > py. Similar trends are observed for the oxidation of Co(II) to Co(III). The complex with X = *N*-MeIm is oxidized at 0.125 V, whereas the oxidation waves for the other complexes are anodically shifted (in the case of complex **12** with X = 2-MeIm, the shift is 170 mV).

Similar behavior is observed for the corresponding phenyl-substituted complexes (A = Ph), with increasingly more negative potentials for the reduction process in the order py < 2-MeIm < Im < NH_3 (complexes **6**, **15**, **13**, and **2**). The phenyl groups lead to an anodic shift of the observed peak potentials E_{pc} for complexes with the same axial ligands by 40−80 mV, thus making the phenyl-substituted complexes easier to reduce. The reason for this is the electron-withdrawing character of the phenyl substituents, which decreases the electron density on the metal center. The para-substituents on the phenyl rings have a significant effect on the observed reduction peak potentials: Electron-withdrawing groups (*p*-FPh, *p*-ClPh) lower the electron density on the metal center even further and lead to less negative potentials than the complexes with electron-donating substituents (*p*-MeOPh). The potentials E_{pc} of complexes with B = Cl are less cathodic (by 225 mV for A = Me and X = NH_3) than those with B = H, suggesting that Cl substituents also remove electron density from the metal.

Equatorial ligand substitutions generally affect reduction potentials less than changes in axial ligands (e.g., the potentials span the relatively small range of 225 mV for complexes with X = NH_3 and different equatorial ligands), a finding that is

(28) pK_a values for the five different axial bases used in this study are (in aqueous solution): py, 5.23; Im, 6.99; *N*-MeIm, 7.25; 2-MeIm, 7.86; NH_3, 10.25. Perrin, D. D. *Dissociation Constants of Organic Bases in Aqueous Solution*; Butterworths: London, 1972; Suppl, 1972.

consistent with electron transfer to d_{z^2} in forming Co(II). It also is of interest that $[Co(salen)(py)_2]ClO_4$ is reduced at a more positive potential (220 mV E_{pc}) than the corresponding acacen complex.[6e] This shift apparently is related to the higher degree of electron delocalization in the Co(salen) unit.

The $Co^{II/I}$(acacen) couples are not influenced by potential axial ligands, which indicates that only four-coordinate species are involved in the electrode reactions. Equatorial substituents affect these potentials in the same way as for Co(III/II) couples. However, while the maximum range of Co(III/II) potentials is only 225 mV (constant axial ligand), the range for the corresponding Co(II/I) couples is 380 mV. The greater dependence of the Co(II/I) couple on the nature of the equatorial ligand is not unexpected,[29] as the lower oxidation states are better electron donors to the π^* orbitals of acacen.

Acknowledgment. A.B. thanks the Alexander von Humboldt Foundation for a postdoctoral fellowship. This work was supported by NSF, the Arnold and Mabel Beckman Foundation, and Redox Pharmaceutical Corp.

Supporting Information Available: Text describing X-ray procedures and tables of X-ray crystallographic data (atomic coordinates, bond distances and angles, anisotropic displacement parameters, hydrogen coordinates) for $[Co(3\text{-}Cl\text{-}acacen)(NH_3)_2]BPh_4$ and $[Co(acacen)(4\text{-}MeIm)_2]Br\cdot 1.5H_2O$ (21 pages). Ordering information is given on any current masthead page.

IC961146V

(29) Tait, A. M.; Lovecchio, F. V.; Busch, D. H. *Inorg. Chem.* **1977**, *16*, 2206.